Bicycle Pedal Isomerization in a Rhodopsin Chromophore Model

Igor Schapiro, Oliver Weingart, Volker Buss

Department of Chemistry, University of Duisburg-Essen, 45141 Essen, Germany

Supporting Information

S1 Cartesian Coordinates

Starting geometry

N	-4.628694333	-0.162713383	-0.306695490
C	-3.314147452	0.259832071	-0.216005978
C	-2.263852796	-0.597326848	-0.069452763
C	-0.982255475	-0.043668136	0.202007364
C	0.119657343	-0.966776695	0.091207399
C	1.506154430	-0.751187284	0.067746227
C	2.258969829	0.498362142	0.477283700
C	3.619460148	0.609792101	0.688673955
C	-0.790294474	1.482070681	0.426947628
C	4.488612906	-0.644448888	0.670434049
H	-4.912982160	-1.188723594	-0.218062011
H	-5.533623597	0.532107481	-0.319837281
H	-3.214586589	1.421395049	-0.126780025
H	-2.415007864	-1.619671611	0.019155693
H	-1.625734447	2.087026706	0.202159816
H	-0.073542171	1.885244076	-0.355233035
H	-0.706855737	1.611598065	1.537176963
H	-0.138765146	-2.053137672	-0.148161530
H	2.107258658	-1.582912600	0.041587293
H	1.643112778	1.412670394	0.508342018
H	4.155817068	1.417950999	0.805739447
H	4.103155714	-1.523218590	0.333613220
H	5.043941621	-0.872410643	1.614929437
H	5.221645007	-0.709535670	-0.005057742

Geometry at the point of surface hopping

N	-4.594734847	-0.359535581	-0.492992366
C	-3.406684241	0.052851602	-0.670515477
C	-2.442729188	-0.452614661	0.130143243
C	-1.093086885	0.145302670	0.281891427
C	0.058849095	-0.548698144	0.061657553
C	1.362538138	-0.494033912	0.602936970
C	2.402474487	0.443624904	0.055498123
C	3.669948382	0.396912481	0.595019595
C	-0.995503812	1.508689193	0.969985696
C	4.139888856	-0.435177277	1.685407363
H	-4.922573049	-1.083442658	0.189937626
H	-5.225783793	0.159238159	-1.094081904
H	-3.167240123	0.872764377	-1.553300704
H	-2.695043575	-1.394106041	0.816553739
H	-1.532297023	1.320741235	2.049991171
H	-1.418490509	2.272771010	0.298398963
H	-0.022224869	1.692863200	1.229057672
H	-0.016759967	-1.501778239	-0.493877855
H	1.624524106	-1.085115648	1.464450078
H	2.179729473	1.076613838	-0.800112096
H	4.513126043	1.059714172	0.416244059
H	3.363508296	-1.132879239	1.936954213
H	4.656386472	-0.030791741	2.608615538
H	4.843650562	-1.382048160	1.359752249

S2 Computational methods

The starting geometry was optimized at a CASSCF/6-31G* level of theory using Gaussian 98[S1]. All 8 π-electrons and 8 π-orbitals of the four double bond chromophore were included in the active space. The trajectory and relaxed scan calculations were calculated using state averaged CASSCF as implemented in MOLCAS 6[S2]. The two lowest roots (equally weighted) were included and the same active space was selected. The single state gradients of the state-averaged wave function were obtained analytically by solving the Lagrange multipliers equations [S3].

In the relaxed scan of the ideal synchronous two double-bond isomerization the bonds C2=C3 and C4=C5 were stepwise equally twisted and kept frozen, whereas the geometry was optimized with respect to all other degrees of freedom. For conrotatory motion C2=C3 was twisted from 180° to 107.5° and C4=C5 from 0° to 72.5° by an increment of 2.5°. In contrast to this the C4=C5 was rotated from 0° to -72.5° in the disrotatory motion.

S3 Conrotatory and disrotatory motions

In case of two double-bond isomerization two different motions lead to the same product. The rotation of the two adjacent double bonds can take place in the same and in the opposite direction which we define as a conrotatory and disrotatory isomerization respectively (Scheme 1). In this context we use the terms to describe the spatial orientation of the rotation. For each of them two permutations exist, e.g. for conrotatory motion both double-bonds can rotate in clockwise and in anticlockwise sense. But since our simulations are carried out in vacuo and no spatial preference exist the permutations are identical.

The torsion angle is defined according to the recommendations of the International Union of Pure and Applied Chemistry (IUPAC)[S4]. In a chain of four atoms A-B-C-D it is a dihedral between the two planes spanned by atoms A,B,C and C,B,D. Using the Newman projection the dihedral angle can be seen as an angle between to bonds defined by the outer atoms. The torsion angle is considered to be positive if the bond A-B is rotated in a clockwise direction through less than 180 degrees in order that it may eclipse the bond C-D. It is negative if this rotation is anticlockwise. However in our study where the a *cis* and a *trans* double bonds are adjacent and have a common single bond which is highlighted in red (see Scheme 1) a conrotatory motion is characterized by a motion of a *cis*-bond from 0° to 180° or -180°and a *trans*-bond from 180° or -180° to 0°. Hence a disrotatory isomerization in our model is defined as rotation of a *cis*-bond from 0° to -180° or 180°and a *trans*-bond from 180° or -180° to 0° respectively.

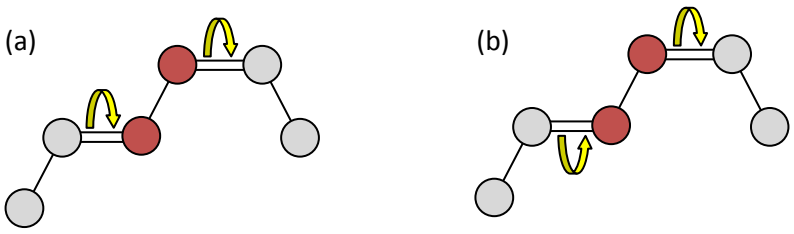

Scheme 1 (a) Conrotatory isomerization and (b) Disrotatory isomerization of an adjacent *cis* and *trans* double bond.

S4 Product distribution

Table S1: product distribution in 47 trajectories of 4-*cis*-pSb grouped by reactive double bond (trajectory with two double bond isomerization excluded). Number of trajectories and ratio in percentage are given for hop events at the first close approach or (in parentheses) for hopping in the direct vicinity of the surface crossing. Details on product determination are described in reference S5.

C2=C3		**C4=C5**	
No. of rotations	*productive*	*No. of rotations*	*productive*
9	9 (6)	37	34 (22)
19%	19% (13%)	79%	72% (45%)

S5 CASPT2 evaluation

On recommendation of one reviewer we extend our calculations to evaluate the effect of dynamic electron correlation on the relaxed scans depicted in Figure 2 of the manuscript. Since geometry optimization at the CASPT2 level is not feasible for our retinal model, we have performed instead CASPT2 calculations along the CASSCF-optimized path (CASPT2//CASSCF) as suggested by the referee.

Figure R1 shows the CASSCF results from Figure 2 in the manuscript complemented by the corresponding CASPT2//CASSCF results (a SA2-(8,8)-CASSCF wave function was used as a reference function and the two lowest roots were considered in the Multi-state CASPT2 as implemented in Molcas 6.4 software; the core orbitals were frozen). From panels A and B it is obvious that at the CASPT2//CASSCF level a conical intersection (CI) is reached neither for the conrotatory nor for the disrotatory pathway. In both rotation modes, the CASSCF ground state potential increases steeply at around 40° twist angle; this increase is missing at the CASPT2//CASSCF treatment although the sigmoid shape of the potential is conserved. In the excited state there are only small differences between CASSCF and CASPT2//CASSCF potentials.

The major difference between the methods is due to the stabilization of the ground state potential at the CASPT2//CASSCF level which leads to a remaining gap between 13 and 15 kcal·mol^{-1} (Panel C). Because at 72.5° the states are almost degenerate at the CASSCF level of theory, rotation and constrained optimization beyond this point up to 90° is not possible; the CASPT2 evaluation was terminated therefore at this point of distortion.

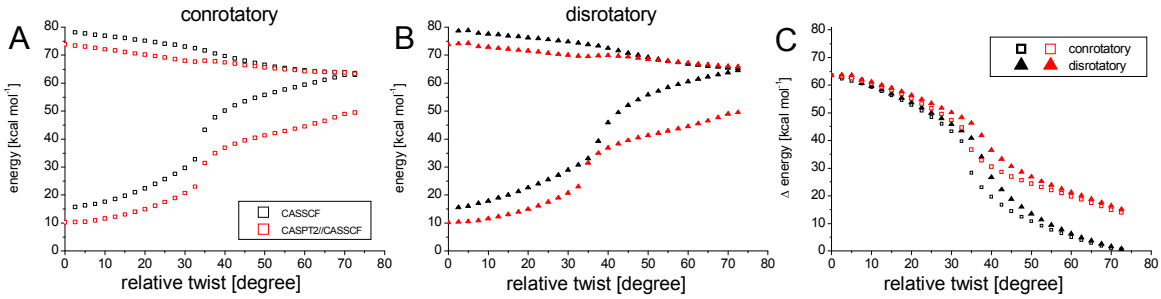

Figure R1. The relative energy of the synchronous conrotatory (A) and disrotatory (B) two double bond isomerization of 4-cis-pSb. CASSCF energies are depicted in black and CASPT2//CASSCF energies in red. The energy of the planar optimized geometry in the ground state is taken as the reference point at the respective level of theory. Panel shows the energy difference between the states S_0 and S_1.

That there remains an energy gap at the CASPT2//CASSCF level is not unexpected: Szymczak et al.[S6] have optimized the CI geometries of short (3-double bond) protonated Schiff bases and found that bond lengths from correlated methods are significantly different from uncorrelated methods. (For similar results see Page et al.[S7] who optimized the geometries of planar-constrained 3- and 5-double bond protonated Schiff bases using CASSCF and CASPT2). So obviously a full optimization is needed which includes all internal coordinates to compare CASPT2 and CASSCF energies to evaluate the importance of dynamical electron correlation, which is not feasible for systems of our size at the present time.

We have also recalculated, with CASPT2//CASSCF, the bicycle pedal trajectory where both double bonds isomerize, as presented in Figure 1 of our manuscript. For the time interval from 20 fs before until 10 fs after surface hopping the CASPT2 energy of each geometry was computed (Figure R2). Panel A of Figure R2 shows what appears to be a general feature, viz. that the ground state is more stabilized at the CASPT2//CASSCF method, especially in the region where the ground and the excited state potentials approach. Also at the time of hopping there is a break of the CASPT2//CASSCF curves.

These findings prompt the question whether the discrepancy between CASSCF and CASPT2//CASSCF is restricted to isomerization of the bicycle-pedal type. We have analyzed 5 trajectories from previous molecular dynamics simulations of the same retinal model where the isomerization occurs around one double bond. The geometries within 5 fs around the hopping time were recalculated. The same methodology was applied as described above. The energy differences for these 5 sample trajectories are shown in Figure R3.

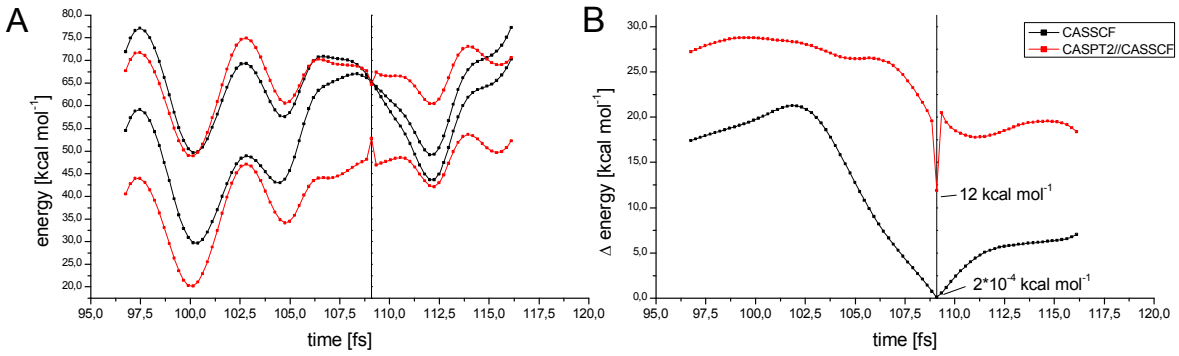

Figure R2. Recomputation of the "bicycle pedal"-trajectory. The energy at the CASSCF level of theory is colored black and CASPT2//CASSCF red respectively. The time of surface hopping is indicated by the vertical line.

Common to the five trajectories is the fact that the energy difference curves at the CASPT2//CASSCF level tend to match at regions far away from the (CASSCF) hopping point. There are large differences, even discontinuities in the hopping region, as observed in panel B of Figure R2, which might be a result of switching to the S_0 level in the CASSCF description at these points. Also the energy gaps are significantly higher. There is only one trajectory (panel A), where the CASPT2//CASSCF treatment indicate a conical intersection: as the CASSCF hopping point is reached, the CASPT2 energy peaks at more than 20 kcal·mol^{-1}; some 3 fs after this the energy is down to less than 1 kcal·mol^{-1}.

These results show that even for the one double bond isomerization a CASPT2//CASSCF treatment is not able to reproduce the hopping geometries found in the CASSCF trajectories, as long as the analytical CASSCF gradients are applied. To explain this one should recall that a return to the ground state via a conical intersection depends on two reaction coordinates as shown by the groups of Robb[S8], Olivucci[S9,S10 ,S11] and Martinez[S12,S13,S14]. The coordinates are the torsion and the stretching mode, especially of the N16-C15 bond. Since we have varied the dihedrals in the relaxed scan at CASPT2//CASSCF level (and therefore one reaction coordinate) the energy difference between the ground and first excited state dropped by 50 kcal·mol^{-1}. But the gap remained larger than at the CASSCF level because the second reaction coordinate was adopted from CASSCF-optimization.

Thus, for a reasonable evaluation of the dynamic correlation effect one should optimize this coordinate at CASPT2 level which is not possible at the moment as already mentioned above. Otherwise it cannot be distinguished whether the difference between CASSCF and CASPT2 is caused by the missing dynamic correlation or by the fact that the geometries were optimized at the CASSCF level of theory. We suggest the remaining 5 to 20 kcal·mol^{-1} as shown by recomputation of trajectories and relaxed scans will be remarkably reduced if this coordinate is relaxed at CASPT2 level.

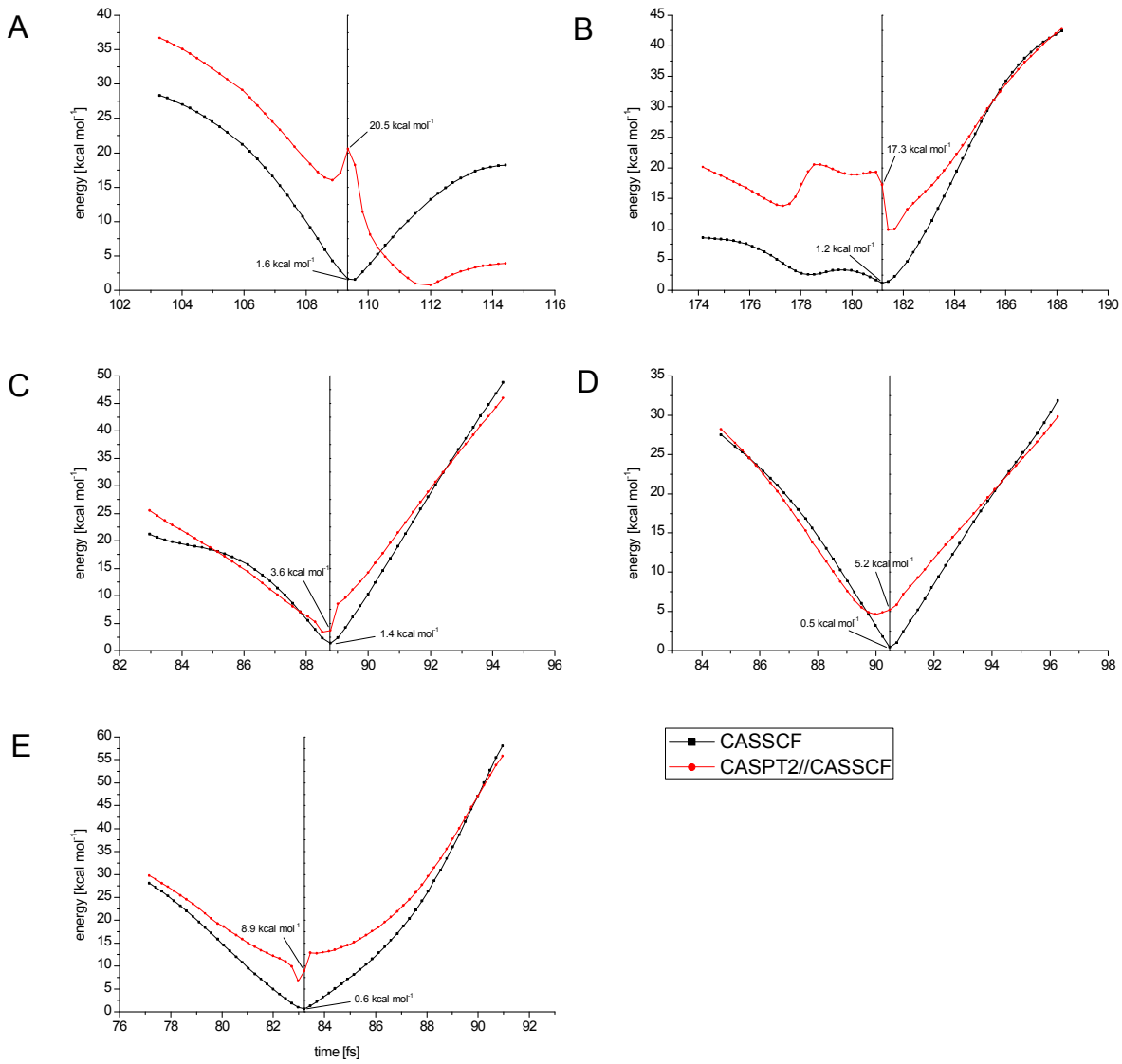

Figure R3. Energy difference $S_1 - S_0$ at the CASSCF (black) and at the CASPT2//CASSCF level (red) around the hopping event for five different trajectories. The vertical lines indicate the time of surface hopping.

We have done the calculations and analyzed in addition a total of 6 trajectories employing CASPT2//CASSCF methodology. We conclude

1) that CASPT2//CASSCF treatment affects both the one and two double bond isomerization in a similar way;

2) that CASPT2//CASSCF is not sufficient to evaluate the effect of dynamic electron correlation in our model because of neglect of geometric parameters, in particular the effect of bond stretching, at the CASPT2 level;

3) that the effect of dynamic correlation exists and should be evaluated but at present the necessary full CASPT2 or MRCISD treatment is not possible.

References

(S1) Frisch, M. J.; Trucks, G. W.; Schlegel, H. B.; Scuseria, G. E.; Robb, M. A.; Cheeseman, J. R.; Zakrzewski, V. G.; Montgomery, J. A.; Stratmann, R. E.; Burant, J. C.; Dapprich, S.; Millam, J. M.; Daniels, A. D.; Kudin, K. N.; Strain, M. C.; Farkas, O.; Tomasi, J.; Barone, V.; Cossi, M.; Cammi, R.; Mennucci, B.; Pomelli, C.; Adamo, C.; Clifford, S.; Ochterski, J.; Petersson, G. A.; Ayala, P. Y.; Cui, Q.; Morokuma, K.; Malick, D. K.; Rabuck, A. D.; Raghavachari, K.; Foresman, J. B.; Cioslowski, J.; Ortiz, J. V.; Baboul, A. G.; Stefanov, B. B.; Liu, G.; Liashenko, A.; Piskorz, P.; Komaromi, I.; Gomperts, R.; Martin, R. L.; Fox, D. J.; Keith, T.; Al-Laham, M. A.; Peng, C. Y.; Nanayakkara, A.; Challacombe, M.; Gill, P. M. W.; Johnson, B.; Chen, W.; Wong, M. W.; Andres, J. L.; Gonzalez, C.; Head- Gordon, M.; Replogle, E. S.; Pople, J.

(S2) Andersson, K.; Barysz, M.; Bernhardsson, A.; Blomberg, M. R. A.; Carissan, Y.; Cooper, D. L.; Fülscher, M. P.; Gagliardi, L.; de Graaf, C.; Hess, B. A.; Karlstro¨m, G.; Lindh, R.; Malmqvist, P.-A.; Nakajima, T.; Neogra´dy, P.; Olsen, J.; Roos, B. O.; Schimmelpfennig, B.; Schu¨tz, M.; Seijo, L.; Serrano-Andre´s, L.; Siegbahn, P. E. M.; Stålring, J.; Thorsteinsson, T.; Veryazov, V.; Widmark, P.-O. MOLCAS Version 6.0; Department of Theor. Chem., Chem. Center, University of Lund, Lund, Sweden, 2003.

(S3) Stålring, J.; Bernhardsson, A.; Lindh, R. Molecular Physics 2001, 99, 103.

(S4) G. P. Moss Pure Appl. Chem., 1996, Vol. 68, No. 12, pp. 2193-2222

(S5) Weingart, O.; Schapiro, I.; Buss, V. J. Mol. Model. 2006, 12, 713.

(S6) Szymczak, J. J.; Barbatti, M; Lischka, H. J. Chem. Theory Comput. 2008, 8, 1189.

(S7) Page, C. S.; Olivucci M. J. Comp. Chem. 2003, 24, 298.

(S8) Garavelli, M.; Vreven, T.; Celani, P.; Bernardi, F.; Robb, M.A. J. Am. Chem. Soc. 1998, 120, 1285.

(S9) González-Luque, R.; Garavelli, M.; Bernardi, F.; Merchán, M.; Robb, M. A.; Olivucci, M. Proc. Natl. Acad. Sci. U.S.A. 2000 97, 9379.

(S10) Garavelli, M.; Celani, P.; Bernardi, F.; Robb, M.A.; Olivucci, M. J. Am. Chem. Soc. 1997, 119, 6891.

(S11) Andruniów, T.; Ferré, N.; Olivucci, M. Proc. Natl. Acad. Sci. U.S.A. 2004 101, 52, 17908.

(S12) Molnar, F.; Ben-Nun, M.; Martinez, T. J.; Schulten, K. J. Mol. Struct. (THEOCHEM) 2000, 506, 169.

(S13) Martinez, T. J. Acc. Chem. Res. 2006, 39, 119.

(S14) Ben-Nun, M.; Molnar, F.; Schulten, K.; Martinez, T. J. Proc. Natl. Acad. Sci. U.S.A. 2002, 99, 1769.